Seismic Assessment of Pipe Racks Accounting for Soil-Structure Interaction

Luigi Di Sarno & George Karagiannakis

International Journal of Steel Structures

ISSN 1598-2351

Int J Steel Struct
DOI 10.1007/s13296-020-00393-7

ONLINE FIRST

Springer

Your article is protected by copyright and all rights are held exclusively by Korean Society of Steel Construction. This e-offprint is for personal use only and shall not be self-archived in electronic repositories. If you wish to self-archive your article, please use the accepted manuscript version for posting on your own website. You may further deposit the accepted manuscript version in any repository, provided it is only made publicly available 12 months after official publication or later and provided acknowledgement is given to the original source of publication and a link is inserted to the published article on Springer's website. The link must be accompanied by the following text: "The final publication is available at link.springer.com”.

Springer

Author's personal copy

International Journal of Steel Structures
https://doi.org/10.1007/s13296-020-00393-7

Online ISSN 2093-6311
Print ISSN 1598-2351

Seismic Assessment of Pipe Racks Accounting for Soil-Structure Interaction

Luigi Di Sarno[1,2] · **George Karagiannakis**[1]

Received: 31 January 2020 / Accepted: 6 August 2020
© Korean Society of Steel Construction 2020

Abstract

The research on the seismic assessment of pipe racks accounting for coupling and soil-structure interaction effects is still scarce. Common industrial practice overlooks critical design aspects due to the insufficiency of current codes that might result in over-conservative or unsafe design. This work addresses the nonlinear analysis of a petrochemical plant steel pipe rack accounting for dynamic interaction with horizontal vessels and pipelines. Soil-structure interaction was evaluated both on pipe rack and pipelines in terms of interstorey-drift ratio and stress–strain response. An attempt was made for correlating the ratio with piping strain to make comparisons with common acceptance criteria for building structures, since code provisions do not address currently limit state design concept for pipe racks. Additionally, seismic fragility curves along with 95% confidence intervals were evaluated for different intensity measures and were used as a tool to demonstrate that the soil deformability could act as an isolation mechanism for pipelines. The increase of pipe rack displacements was an additional impact of soil, though, it was not as much profound as on the seismic response of the pipelines. The detailed structural assessment through extensive nonlinear dynamic analyses demonstrated that the return period of exceedance of pipe rack and pipelines limit state, considering the median spectral acceleration as a measure, occurred 1.84 and 2.64 greater than the design one, and this might be an indication that the performance-based concept should be applied for pipe rack systems to achieve a safe, risk-consistent among structural and nonstructural members and cost-effective design.

Keywords Seismic design · Steel pipe rack · Dynamic interaction · Fragility assessment · Seismic assessment · Interstorey drift · Pipe strain · Petrochemical plant

1 Introduction

Pipe Racks (PRs) are non-building systems similar to building critical structures inside oil refineries that support Piping Systems (PSs), e.g. vessels and pipelines at multiple or a unique level due to process, maintenance, safety, financial and other reasons. Such structures may present similar behaviour to buildings, since they comprise moment or bracing resisting frames (with partially or fully-restrained connections) as lateral resisting system. However, supporting non-building structures and non-structural elements could result in high irregularities in plan and elevation due to uneven masses among stories, stiffness and/or strength distribution. These irregularities may cause complex seismic response of PRs with respect to common buildings, let alone when Soil-Structure Interaction (SSI) is accounted for in the analysis. Oil refineries are located at coastal site, where the supporting soil is usually weak, hence the seismic response could become even more complex, considering that soil may have a significant impact on PR–PSs. Due to the structural complexity and importance for the smooth operation of process plants, design aspects for PRs such as the dynamic interaction of supported equipment with the supporting structure, performance-based design and the SSI effects should further be investigated.

First, modelling difficulties can arise when dealing with structural and nonstructural members, since analysis software are either structural or piping engineering oriented. The nonlinear geometry of equipment and consideration of material nonlinearity make it particular difficult structural members and nonstructural components to be analysed together. Also, the European seismic code EN1998-1 (2004)

✉ Luigi Di Sarno
ldisarno@unisannio.it

[1] University of Sannio, Benevento, Italy

[2] University of Liverpool, Liverpool, UK

Published online: 13 August 2020

Author's personal copy

postulates that the dynamic coupling can be ignored using equivalent static methods that might underestimate differential displacements, which is one of the most predominant failure mode of pipes. The research of Azizpour and Hosseini (2009) demonstrated that the dynamic properties of a steel rack could considerably be changed with respect to pipelines weight, rigidity of connections and boundary conditions at pipes edge that bring the code prescriptions into question, since they account mainly for the weight ratio between nonstructural components and supporting structure, and thus neglect the local modes of multiply-supported pipes.

Secondly, the limit-state design has not applied to PR–PSs yet, given that seismic codes still postulate the use of allowable stress method for pipelines. Using this design method, beam elements instead of rigorous shell elements can be adopted for pipes, keeping both PR and PS below the yielding point. Also, the literature is still very scarce on this topic. A PS was modelled with beam elements and coupled with a steel PR in Bursi et al. (2016). Designing the piping according to allowable stress design method and then assessing it through time-histories of seismic level corresponding to predefined Limit States (LSs), the research demonstrated the over-conservativeness of the design method. In particular, the rack presented some mild inelasticity on the braces, though, the PS remained quite below the yielding point even at Safe Shut-down Earthquake (SSE). Another research that shed light on traditional prescriptive design of these systems was done by Di Roseto et al. (2017). The fragility of a stiff and a flexible code-conforming PR with the same layout and without accounting for dynamic interaction with pipelines was derived. It was illustrated that the stiff rack -this type is commonly adopted in the oil and gas industry- was highly conservative against plasticity and could be unsafe due to high peak floor acceleration that could damage supported pipework, as it was also found in the work of Di Sarno and Karagiannakis (2019).

As far as soil deformability is concerned, it has been shown that SSI may have significant impact on stiff and squat structures e.g. nuclear containments, storage tanks or braced structures by lowering force demand and increasing lateral displacement; however, the opposite may also apply for certain seismic and soil environments (Mylonakis and Gazetas 2000). A nuclear reactor was examined in Wang et al. (2017) and it was deduced that SSI could diverge the response spectra from the fixed-base case and increase the spectral acceleration at higher floor levels, which was critical for components attached at these floors. On the other hand, the investigation of a four story steel frame structure coupled with equipment at the top floor was conducted by Zhang and Jiang (2017) accounting for SSI, and the results demonstrated the decrease of acceleration, shear and displacement response of both equipment and steel frame; however, the influence was dependent on seismic record variability and intensity. In the same vein, Raychowdhury and Ray-Chaudhuri (2015) demonstrated the beneficial effects of soil on nonstructural components mounted as single-degree-of-freedom systems on a four storey steel moment resisting frame around the first fundamental period of the building. Also, it was observed that the structural nonlinearity may increase the response of the components near the second and third fundamental period of the steel frame, which was no more obvious when the SSI was considered.

To the best of Authors' knowledge, there is no research that addresses the nonlinear seismic response of pipe rack—piping systems accounting for dynamic coupling, SSI effects as well as more advanced piping modelling. The seismic assessment of these structures could pave the way towards adopting a performance-based design that could be communicated more effectively to stakeholders and result also in material saving. To this effect, a sound performance-based assessment of a petrochemical steel pipe rack is conducted in the following and comprises 6 main steps (Fig. 1). First, the analysis software is selected based upon the model requirements such as pipelines nonlinear geometry, soil modelling as well as plasticity models of structural members and pipelines. Secondly, the fragility analysis method (either static or dynamic) is selected considering the seismic response of PR–PS. For instance, a PR that supports rigidly a heavy equipment and is governed by the first fundamental mode can be assessed as a single degree-of-freedom model using static pushover analysis, though, dynamic analysis can be a more adequate option when higher modes and irregularities exist. Also, if PR–PSs are analysed as decoupled and the multiple-support excitation is used for the PS, the incremental dynamic analysis may not be the best option due to the excessive computational cost. It should be emphasized that the analysis method should be compatible with the analysis code that was selected in the previous step. In case dynamic analysis is adopted, seismic records are selected (step 3) either with uniform hazard spectrum as the current European codes specify or using the conditional spectrum approach, which is a widely accepted method for seismic assessment in the literature. It should be mentioned that considering the envelope of the spectra of various seismic records, as the uniform hazard method does, may be more preferable for irregular structures with higher mode effects. The fourth step regards the identification of main failure modes for PRs, e.g. failure under axial load, shear, bending or combined actions due to equipment oscillation, or for pipelines e.g. buckling of pipes due to differential movements between adjacent supports. Finally, performance levels and damage states are defined (step 5) to be used for evaluating the fragility of the system, and subsequently estimating the mean annual frequency of exceedance (step 6) both for structural and non-structural elements using statistical methods

Author's personal copy

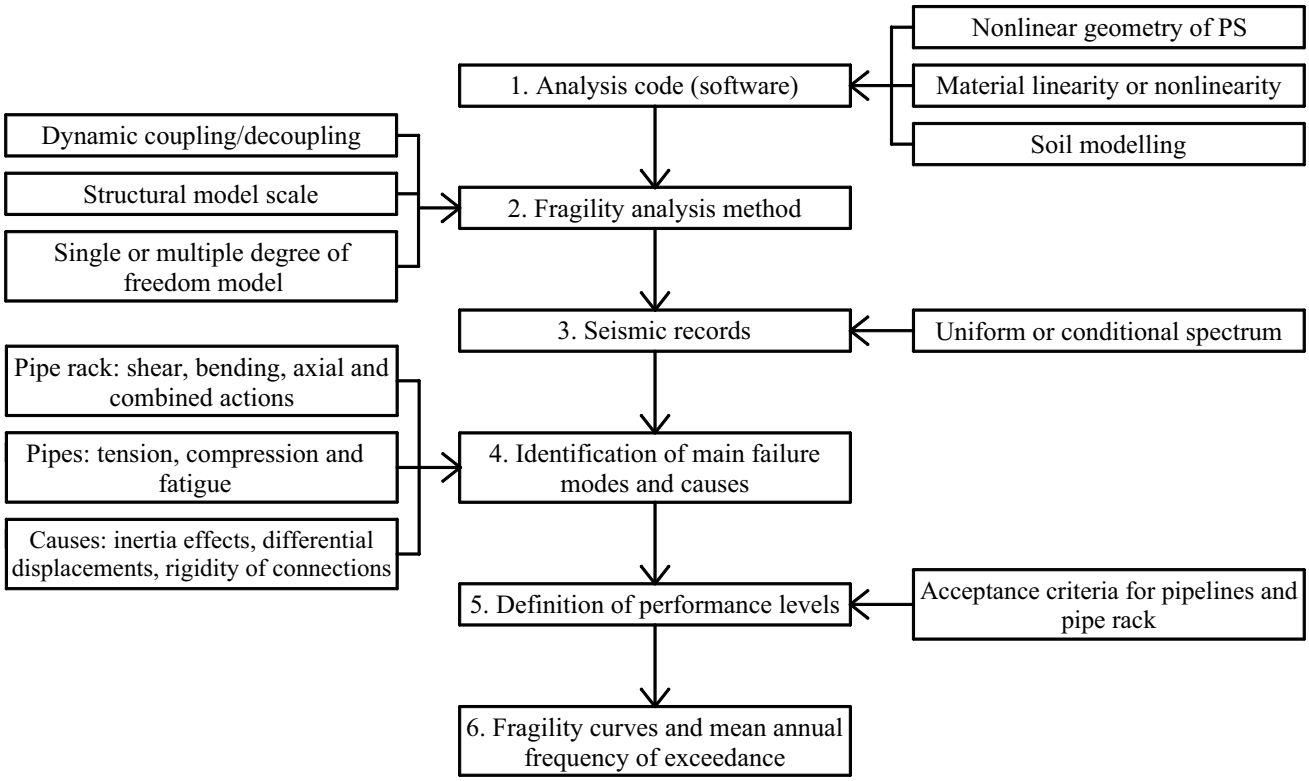

Fig. 1 Flow-chart diagram of PR–PS fragility assessment

compatible with the analysis one e.g. fractiles or maximum likelihood. The return period of violating a certain limit state is a tangible estimate that can be communicated to stakeholder for decision making and in this Case Study (CS) is used to evaluate the code conservativeness. The steps 1–2 have been already described in Di Sarno and Karagiannakis (2019), thus the present study will focus mainly on steps 3–6 by addressing the same CS.

2 Model Description

2.1 Pipe Rack and Piping Configuration

Distribution systems that outfit PRs should be flexible enough, particularly in seismic prone regions, to accommodate high displacements and reduce seismic forces, stemming from the supporting structure. Flexible/expansion loops with pipe bends are formed for this purpose (Fig. 2), and were also adopted for the following CS. Supporting systems are usually stiff compared to pipelines stiffness and the last are mainly considered as partially/totally unrestrained in the longitudinal direction. This support mechanism is designed to act as fuse to pipelines response, thus it is up to structural and piping engineer where a pipe will present the

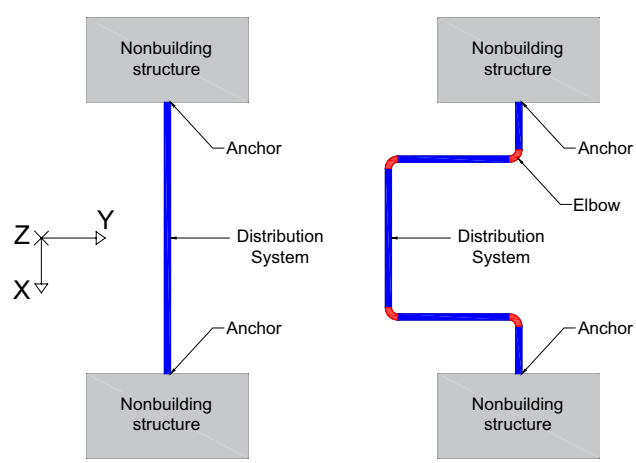

Fig. 2 Schematic representation of system flexibility distribution

most critical response in order to reduce the probability of failure occurrence.

The analytical model being examined hereafter pertains to a concentrically braced steel pipe rack that supports a piping system, which constitutes two horizontal vessels and a unique pipeline (Fig. 3). The selection of ABAQUS (2017) software comes after its rigorousness for nonlinear material and geometry characterisation e.g. pipe bends. The steel PR is modelled with B31 linear

Author's personal copy

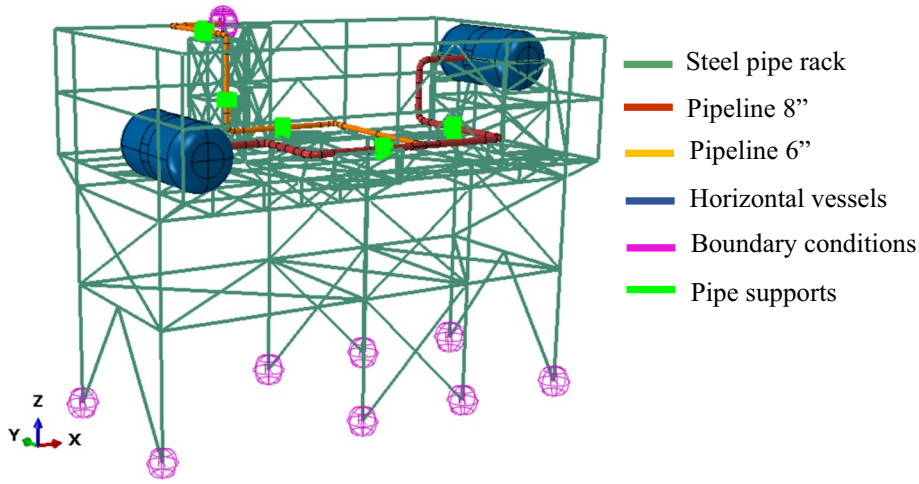

Fig. 3 The steel pipe rack and supported piping system without soil-structure interaction

beam elements in space. The PR consists of different HEB and IPE section profiles as well as circular or rectangular concentric bracing (X-crossing or inverted V) in vertical and horizontal direction. Elastoplastic steel of S275 grade with isotropic strain hardening is considered. As it was stressed out above, to make the system more flexible, the pipeline bents at several points in order to finally run into a nearby unit. The PS includes a unique pipeline of 8″ diameter, which connects two horizontal vessels, and then reduces to 6″ diameter running up to a nearby unit. The edge of the pipe is considered as fixed on the tower. The pipe material refers to an elastic perfectly plastic steel with 418 MPa and 554 MPa yielding and ultimate strength, respectively. Given the small scale of the system and the need to achieve higher accuracy compared to beam elements, the straight pipes are modelled with 4-node and reduced integration shell elements (S4), whereas the pipe bends with S3 general-purpose triangular shell elements. The PS dynamic properties have been verified with experimental results (DeGrassi et al. 2008) and other numerical studies (Bursi et al. 2015). Additional information about the geometrical and mechanical properties of the system could be found in Di Sarno and Karagiannakis (2019).

There are several uncertainties when dealing with the seismic response of these systems; apart from the seismic input, modelling ones regarding mainly to boundary conditions, pipelines and vessels support, pipelines layout and type of pipe elements are essential in order to be assessed reliably. The consideration of linear elastic behaviour accounting for beam elements for pipelines, which is usually adopted in the industry, intends to reduce the number of uncertainties. However, to acquire a better insight compared to linear response, which has been considered within the rather few research in the literature, the behaviour of the system is examined in the nonlinear regime.

2.2 Soil-Structure Interaction

To take the effects of soil deformability into account, the pipe rack is supported by a raft foundation. This choice relies upon the high demand for differential movements avoidance due to the unsymmetrical support of tanks (mass irregularity) on the third floor. The foundation is made of concrete C40/50 with 0.30 m thickness considering eight-node brick elements of reduced integration. Six equivalent soil springs in each of the six degrees of freedom are calibrated and placed at the foundation centre of gravity to represent the soil medium below the foundation (Fig. 4a). The calculation of stiffness springs could be done based upon different

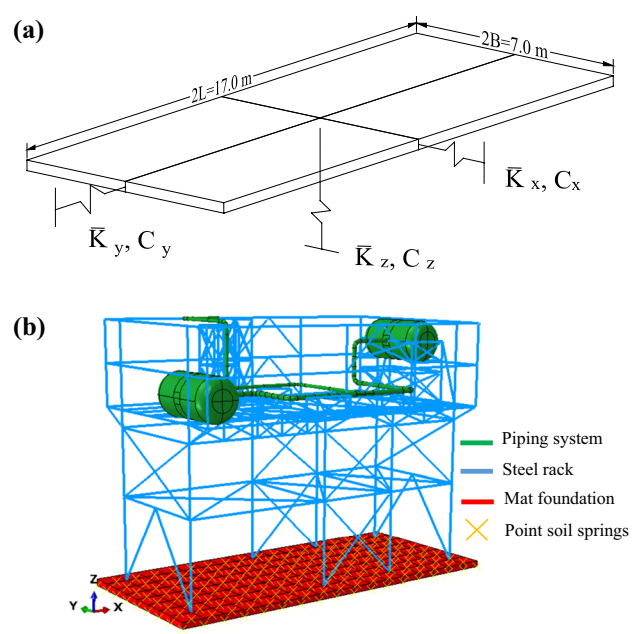

Fig. 4 Soil-structure interaction for a steel pipe rack **a** the mat foundation with the lumped spring in the center, **b** perspective view of pipe rack coupled with the PS and distributed soil springs

Author's personal copy

methods; in this CS, the Winkler spring model was adopted due to its efficacy in previous studies and standards (e.g. FEMA 356 2000; Dutta et al. 2009; Elnashai and Di Sarno 2015).

The formulation of static stiffness is achieved after Gazetas (1991) and refers to a lumped spring attached to a rigid and massless foundation resting on a homogeneous elastic half-space (Fig. 4a). The frequency of ground excitation could impact the spring stiffness, and this is the reason for multiplying the static stiffness with a multiplication factor that is commonly plotted as a function of the non-dimensional parameter a_0 $(=\omega \times B/V_s)$. The looser the soil or the larger the length-to-width ratio (L/B), the greater the influence of the factor on the dynamic stiffness. Although the dynamic stiffness with respect to the first principal pipe rack mode of the compliant structure is considered in this study, the factor was not considerably high due to the relatively low ratio (L/B). Several studies have also shown that the influence of frequency-dependent stiffness of springs is not considerable within the range of parameters of interest for structures (Bhattacharya et al. 2004; Dutta et al. 2009). Finally, elastic springs and dashpots accounting both for radiation and hysteretic damping of soil are introduced in two horizontal (denoted as x and y) and vertical z-direction, and then distributed as point springs at 1 m intervals below the raft foundation as shown in Fig. 4b. The springs at the sides and corners are calibrated by introducing the half and quarter, respectively, of the stiffness and damping of the internal ones, since they regard to smaller surface area. Considering that oil industrial plants are commonly rested on alluvium deposits, a sandy clay to clayey sand is selected. The soil pertains to C type as categorised in EN1998-1 (2004) based upon the average shear wave velocity in the top 30 m. The mechanical soil properties as well as the stiffness and dashpots of springs in the three horizontal directions are quoted in Table 1. Also, the period elongation for four principal period of the PR along with the decrease in mass participating ratio are listed in Table 2.

Table 1 Soil properties and spring horizontal stiffnesses considered

Shear wave velocity, $V_{s,30}$ (m/s)	210
Shear modulus (MPa)	108
Density (t/m^3)	1.76
Poisson ratio, ν	0.33
K_X (kN/m/m^2)	26,426
K_Y (kN/m/m^2)	28,527
K_Z (kN/m/m^2)	34,066
C_X (kN × s/m/m^2)	370
C_Y (kN × s/m/m^2)	370
C_Z (kN × s/m/m^2)	568

Table 2 Principal periods of the rack without (W/O) and with (W/) SSI

Mode	T (s)		M (%)	
	W/O	W/	W/O	W/
2	0.440	0.502	42	30
6	0.312	0.331	26	19
12	0.233	0.242	15	12
5	0.282	0.286	10	7

3 Performance-Based Assessment

3.1 Limit States for PR–PSs

The concept of seismic performance-based design regards the design of a structure to perform for a predefined level e.g. Serviceability, Safe Life or Collapse Limit State (SLS, SLLS or CLS) given an earthquake with a certain seismic intensity (Fig. 5). Petrochemical plants are considered as critical facilities, thus they are designed for an earthquake with higher and lower return period compared to common building structures and highly critical power plants, respectively. NTC (2018) accounts directly for higher return period by multiplying the response spectrum by the factor γ_{IC}, which is equal to 1.5 in case of industrial facilities (see more information in Di Sarno and Karagiannakis 2019). The present PR was designed for the SLLS and earthquake with probability of occurrence equal to 6.8% in 50 years or 713 years return period. It pertains to design spectral acceleration, $S_{aR,d}$ and $S_{aP,d}$, equal to 0.67 g for the PR and 0.59 g for the PS, respectively. This seismic level was correlated with Operating Basis Earthquake (OBE) for the design of

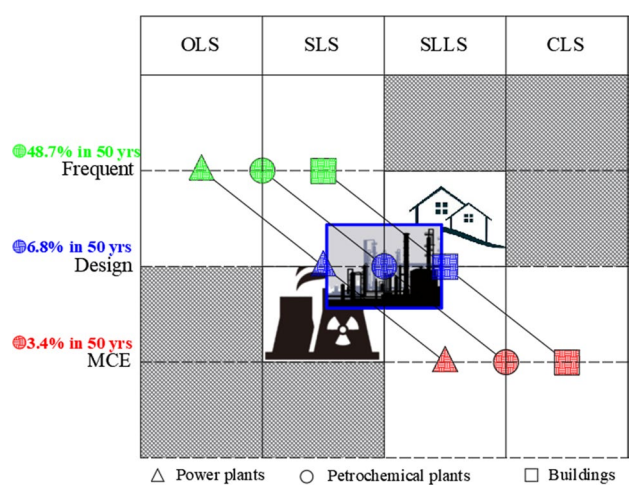

Fig. 5 The concept of performance-based design adopted for the petrochemical plant pipe rack

Author's personal copy

the PS as postulated in EN13480-3 (2012), which refers to design peak ground acceleration, PGA_{OBE}, equal to 0.26 g. Designing the piping system in a code-conforming way still requires the application of the conservative allowable strain method, which keeps the pipes below the yielding point and makes the PR even stiffer. To this effect, the PR was designed to appear some mild inelastic deformation, which is reflected as having *IDR* mildly greater or lower than 0.5%. To stress out the conservativeness of current design codes for PR–PSs, the maximum considered earthquake (MCE) is also stressed out in the following assessment, which pertains to 3.4% probability of occurrence in 50 years or 1425 years return period and regards to SSE in EN13480-3 (2012) with $PGA_{SSE} = 1.5 \times PGA_{OBE}$.

The horizontal vessels governed the response since they constituted roughly 60% of the total weight of the system and caused the rack to fail under bending on the upper floor. The importance of vessels vibration on system behaviour was demonstrated in Di Sarno and Karagiannakis (2019) by comparing the capacity curves derived through static and dynamic analysis, where the former yielded considerably higher resistance, since the mass of the vessels was not activated. The specification of performance levels along with damage states is the penultimate step of fragility assessment of PRs as demonstrated in the flow-chart above (Fig. 1), which is as much crucial step as the previous ones. In case of PR–PSs, apart from specifying damage states for structural members, acceptance criteria should be defined for the non-structural elements. The seismic response of the system was assessed by using Interstorey Drift Ratio (IDR) as an Engineering Demand Parameter (EDP). Typical values of *IDR* for steel structures are reported in Elnashai and Di Sarno (2015). Limit states for pipelines are commonly based on engineering judjment and the degree of conservativeness. There are three main failure modes of pipelines, viz failure under tension, compression (local buckling) and fatigue. Although, the last mode has been reported as equally crucial for pipelines (Vathi et al. 2017), only the first two modes were examined in this CS. The fatigue failure mode is correlated with the buckled area of pipe due to compressive strain and occur due to strong repeated loading in that area after reaching the ultimate resistance. Therefore, assuming ultimate resistance of pipe ε_{Cu} equal to 1.6% and 1.9% for the 8″ and 6″ nominal pipe sizes, respectively, is on the safe side considering that a pipe that has a buckled area is rather vulnerable and needs replacement, even if loss of containment event has not occurred. More information about damage states for pipelines can be found in Vathi et al. (2017). Since the PR–PS were analysed on rigorous finite element analysis program ABAQUS (2017), it was found easier to examine the plasticity development on pipes by using the scalar measure *PEMAG* (plastic strain magnitude). Thus, the ultimate resistance for both compression and tension, which pertained to Collapse Limit State (CLS), were compared, and the lowest between the two was adopted for the assessment as shown in Table 3.

3.2 Assessment of System Behaviour with SSI

To assess the system performance towards shedding some light on pipe racks design requirements and demonstrating whether the current code provisions are conservative or not, the PR was analysed accounting for coupling with the PS as well as SSI. The seismic fragility of the system was evaluated using 20 seismic records that can be found in European Strong-motion Database (ESD). The records are compatible with NTC (2018) or EN1998-1 (2004) type 1 spectrum in both directions (Fig. 6a, b). Both near- and far-field conditions were considered with epicentral distance between 3 and 94 km. To reduce the computational cost, a bracketed duration was used for each record. More information regarding the selected records can be found in Table 4.

Before assessing the fragility of the system, it was found preferable to illustrate the PR seismic behaviour in terms of *IDR* for some representative records without (W/O) and with (W/) SSI effects. The *IDR* time-histories for two different seismic levels (OBE and SSE) and same record (Rec1) are illustrated in Fig. 7a and b. The increase of *IDR* was obscure both for OBE and SSE level when accounting for SSI. The time-histories of Rec 2 were compared for the X and Y direction (Fig. 7c and d), since it was found in Di Sarno and Karagiannakis (2019) that the system reserved higher strength in the X direction. The increase of the maximum IDR value was greater in the most flexible direction (Y), however, the difference was not considerable at SSE level. This behaviour could be attributed to the high resistance of system in both directions. Finally, the *IDR* time-history of Rec2 was evaluated for seismic intensity around 4 times the SSE level, and eventually, the influence of SSI was more considerable in both directions e.g. roughly 50% in the X and nearly 25% increase in the Y direction, as shown in

Table 3 Acceptance criteria for pipe rack and piping system

EDP	Limit states	Damage states
IDR (%)	OLS	$d/h < 0.2$
	SLS	$0.2 < d/h \leq 0.5$
	SLLS	$0.5 < d/h \leq 1.5$
	CLS	$1.5 < d/h \leq 3$
Plastic strain, ε (%)	OLS	$\varepsilon < \varepsilon_y^a$
	SLS	$\varepsilon_y < \varepsilon \leq 2.5 \times \varepsilon_y$
	SLLS	$2.5 \times \varepsilon_y < \varepsilon \leq \varepsilon_{Cu}^b$
	CLS	$\varepsilon \geq \varepsilon_{Cu}$

[a] $\varepsilon_{y=}$pipe yielding strain

[b] ε_{Cu} is different for pipe 6″ and 8″

Author's personal copy

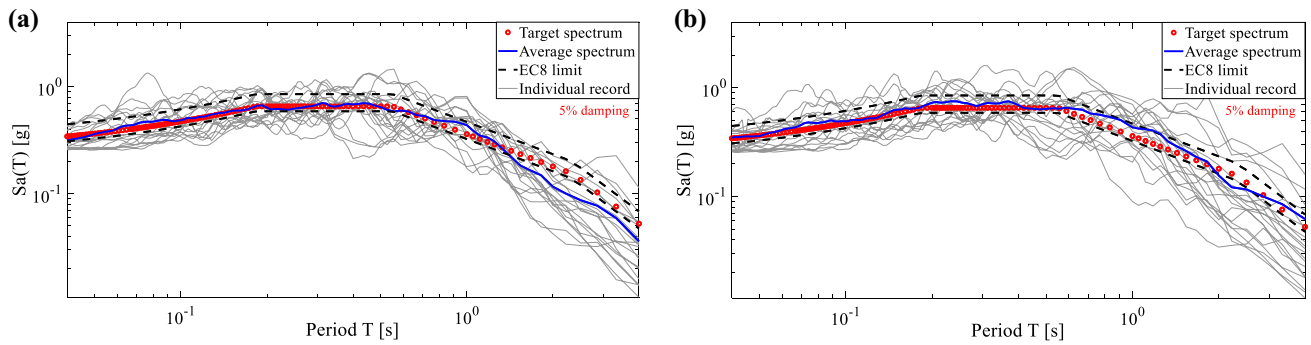

Fig. 6 The response spectra of the selected ground motions in a. X and b. Y direction

Table 4 The seismic records considered for the assessment of dynamically coupled system

Rec#	Earthquake name	Date	M_W	Epicentral distance (km)	PGAX (g)	PGAY (g)	Bracketed duration[a] (s)	Predominant period (s)
1	Faial	09/07/1998	6.1	11.00	0.420	0.382	8.42	(0.476, 0.37)
2	Spitak	07/12/1988	6.7	36	0.18	0.18	10.75	(0.303,0.357)
3	Banja Luka	13/08/1981	5.7	7.00	0.442	0.404	6.00	(0.119, 0.080)
4	Manjil	20/06/1990	7.4	91	0.13	0.21	14.27	(0.294,0.303)
5	Pyrgos	26/03/1993	7.2	1.00	0.102	0.188	5.50	(0.104, 0.172)
6	UMarche	26/09/1997	6	5	0.20	0.22	12.14	(0.185, 0.090)
7	Dinar	01/10/1995	6.4	8.00	0.273	0.319	26.40	(0.303, 0.345)
8	Adana	27/06/1998	6.3	30	0.22	0.27	8.56	(0.667, 0.500)
9	UMarche	26/09/1997	4.3	3.00	0.345	0.261	7.62	(0.179, 0.345)
10	Izmit	17/08/1999	7.6	94	0.18	0.16	5.67	(0.556, 0.370)
11	Duzce	12/11/1999	6.0	5.27	0.525	0.414	23.57	(0.417,0.345)
12	Patras	14/07/1993	5.6	37	0.02	0.03	11.13	(0.435, 0.172)
13	Miyagi	27/07/2003	5.8	9.93	0.199	0.257	20.00	(0.114, 0.132)
14	UMarche	14/10/1997	5.6	13	0.09	0.07	5.26	(0.152, 0.312)
15	Abruzzo	07/05/1984	5.9	45	0.06	0.06	7.04	(0.455, 0.588)
16	Izmit	17/08/1999	7.6	92	0.09	0.10	7.56	(0.667, 0.667)
17	Izmit	17/08/1999	7.6	39	0.09	0.13	10.63	(0.370, 1.180)
18	Cubuklu	20/04/1988	5.5	34	0.04	0.05	7.58	(0.333, 0.769)
19	Strofades	18/11/1997	6.6	69	0.05	0.05	12.20	(0.263, 0.161)
20	Ishakli	03/02/2002	5.8	35	0.04	0.05	6.12	(0.179, 0.323)

[a]: bracketed duration so that the response spectrum within the interval of interest remains the same

Fig. 7e and f. The impact of tank vibration (or tank bouncing) caused PR to behave in the inelastic region, and this may be a reason for the greater influence of SSI at higher seismic intensity.

The consideration of soil deformability was proved a considerable parameter for the system performance, since it decreased considerably the stress–strain development on pipes. The response of the system for Rec1 scaled at SSE level W/O and W/SSI is illustrated in Fig. 8. The former case caused the maximum stress on PS joint (308 MPa), whereas the latter reduced considerably the stress on PS and relocated the point of maximum stress to the PR (Fig. 8a, b). The stress distribution on T-joint for both cases is illustrated in Fig. 8c and d.

The time-history of pipe stress was evaluated on T-joint (Fig. 9a) and anchor (Fig. 9b) for SSE seismic level of Rec1 and Rec2, and it could easily be noticed that the maximum stress reduced by 45% and 40%, respectively. This outcome of pipe stress reduction due to SSI may be useful in the future within the performance-based design framework of PRs towards reducing excessive cross sections of structural members due to displacement requirements of PS. Another way to realise the beneficial effects of SSI on pipelines could be by looking at maximum plastic strain development on

Author's personal copy

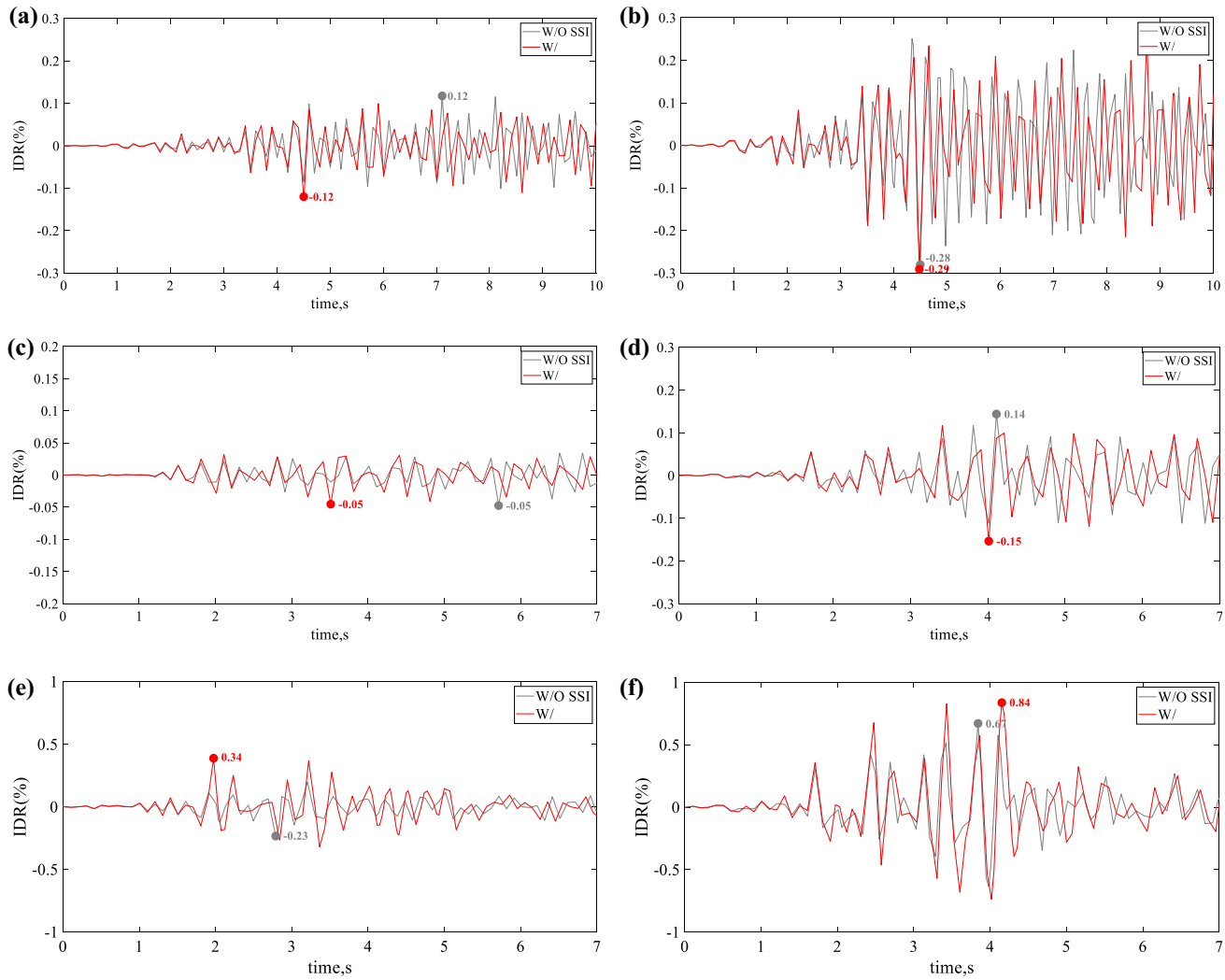

Fig. 7 Comparison of IDR time history W/O and W/SSI for **a** OBE and **b** SSE level (Rec1), **c** in X- and **d** in Y-direction at SSE level (Rec2) as well as **e** in X- and **f** in Y- direction at 4 times the SSE level (Rec2)

T-joint at SSE level of Rec3 (Fig. 10). For instance, the strain reduced considerably from $0.64 \times \varepsilon_y$ to $0.30 \times \varepsilon_y$ as shown in Fig. 10a–c. The reduction of plastic strain on T-joint for Rec4 was estimated at 36% as illustrated in Fig. 10d.

Since PRs are always coupled with equipment and the integrity of the system depends on the performance of both structural and nonstructural elements, the demand of the former should be correlated with the latter to acquire a better insight of system safety level. For instance, if a rack has exceeded the *IDR* limit for SLLS, although the pipes are still safe, it is reasonable that the system cannot be considered operational in reality. Assumptions that regard the sequence of failure appearance may be important for a quantitative risk assessment by assuming loss of containment event and pertinent costs for rack retrofitting or pipes replacement. First, the seismic intensity in terms of normalized *PGA* to design PGA_{OBE} is depicted as a function of *IDR* in Fig. 11. Concerning the case W/O SSI (Fig. 11a), it could be seen that the median *IDR* is 0.32% and 0.40% at OBE level and SSE level, respectively, which means that PR did not exceed the SLLS even at SSE yet at 2 times the OBE seismic level. This outcome indicates the high overstrength that the system reserves. When the SSI was considered, the IDR increased slightly for the two seismic levels (Fig. 11b), as mentioned above.

Furthermore, the relationship between the seismic intensity with the pipe plastic strain is illustrated in Fig. 12a and b. The strain was found 69% of the ε_y and decreased at 50% when the soil deformability was accounted for. Since the strain was lower than the yielding value at SSE level, it means that the PS, in contrast with the PR, did not exceed the SLS even at such high seismic intensity. The pipelines reached the SLS at 1.63 times the PGA_{OBE}, which increased substantially by almost

Author's personal copy

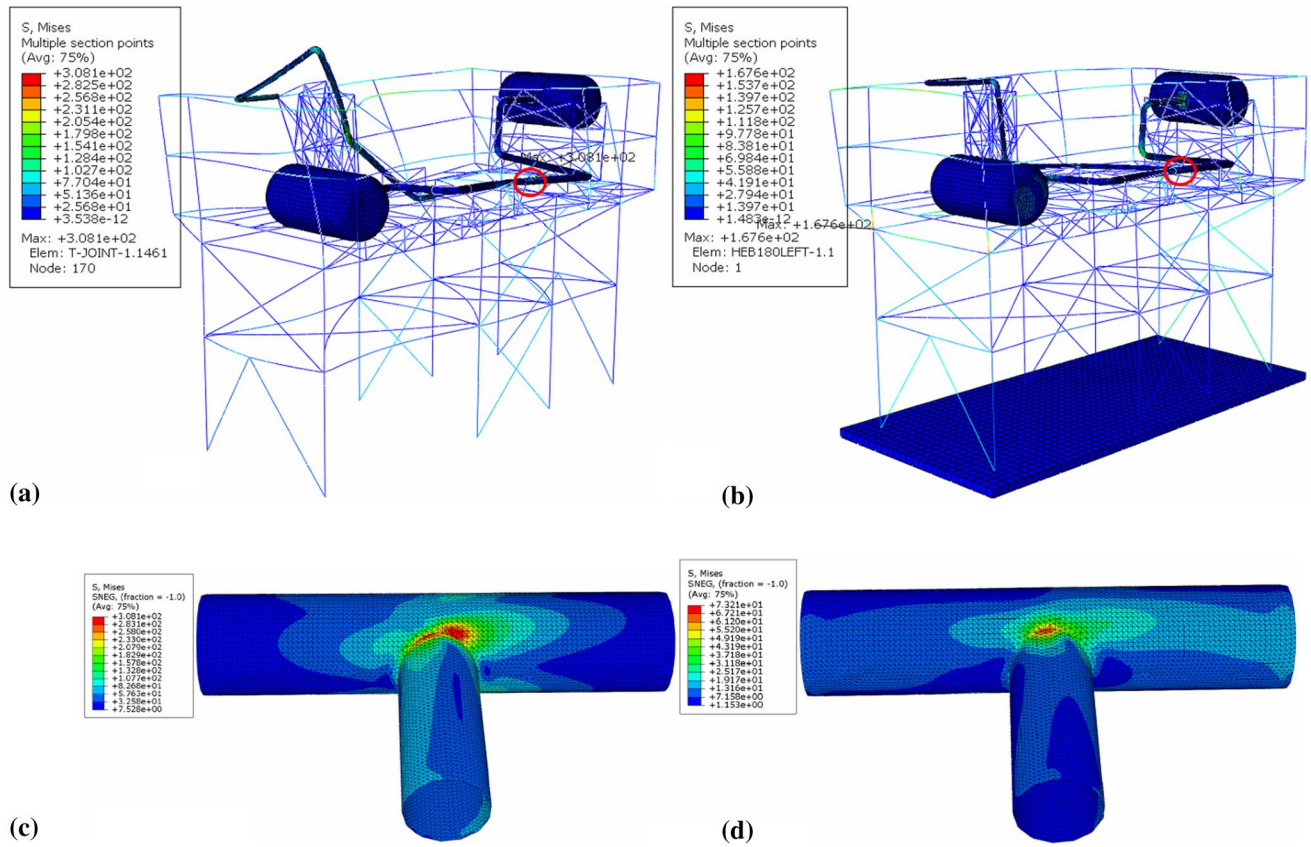

Fig. 8 The stress development for **a** system W/O SSI, **b** system W/SSI, **c** T-joint W/O SSI and **d** T-joint W/SSI referring to the same seismic record (Rec1) and time frame at SSE level (T-joint is circled)

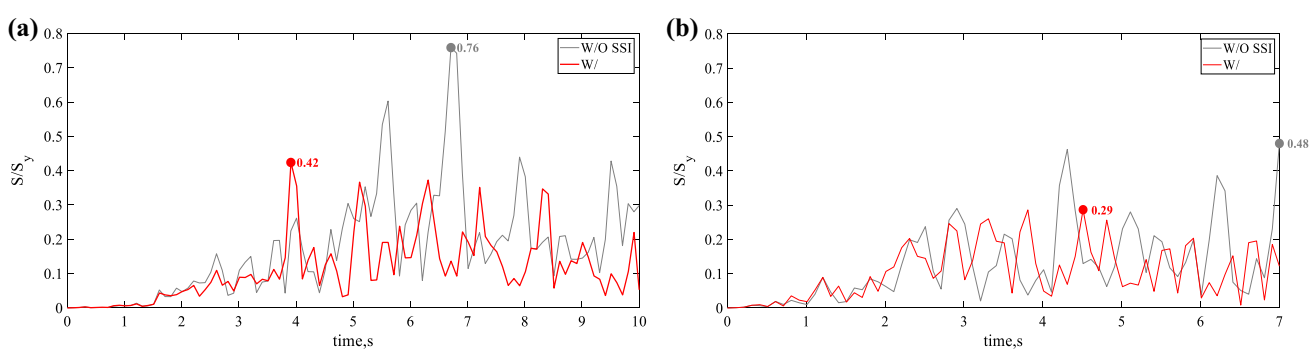

Fig. 9 The effects of SSI on the seismic response of **a** T-joint and **b** anchor for Rec1 and Rec2 at SSE level

25% when accounting for the beneficial impact of SSI. Overall, it could be deduced that the SSI had a greater impact on PS than the PR and the system did not present the seismic behaviour of a common building, since *IDR* value remained below SLLS (for which it was designed for) even at $2 \times PGA_{OBE}$.

4 Seismic Fragility Assessment

A Fragility Function (FF) describes the probability of exceedance of a certain LS of a system or a component that is evaluated in terms of an EDP given an Intensity

Author's personal copy

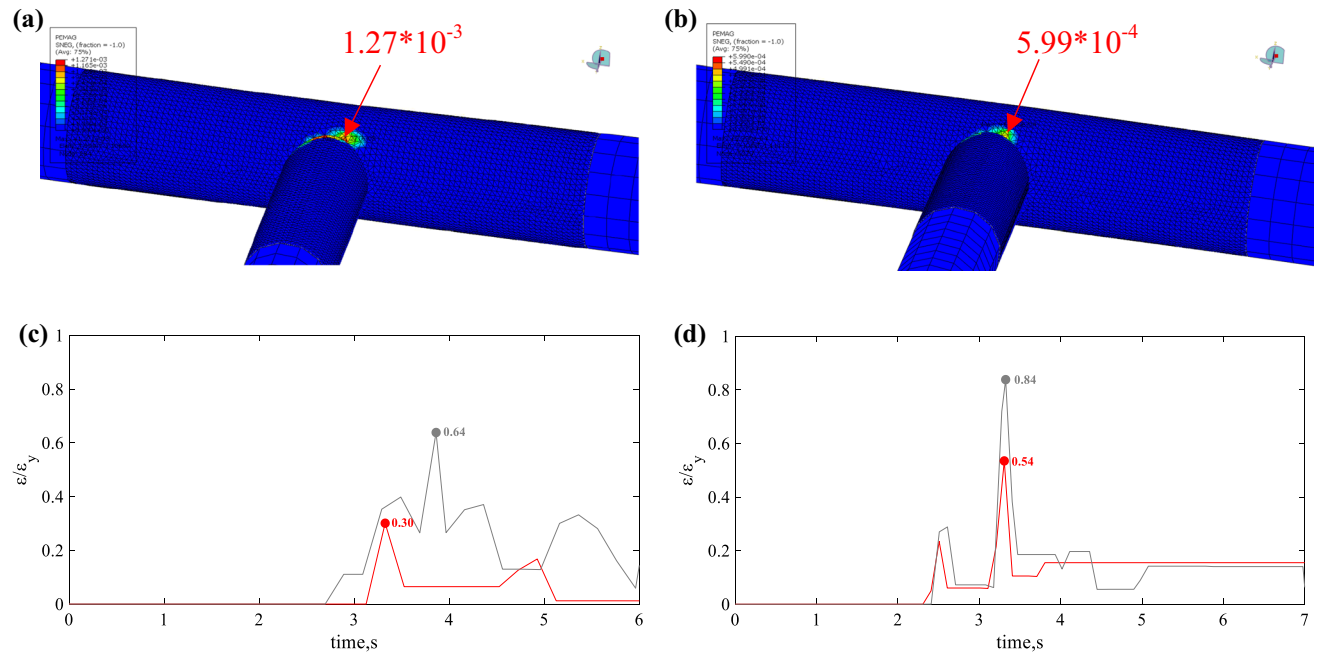

Fig. 10 The location of maximum plastic strain on the PS (T-joint) for Rec3 a. W/O and b. W/SSI as well as the history of magnitude of plastic strain for **c** Rec3 and **d** Rec4

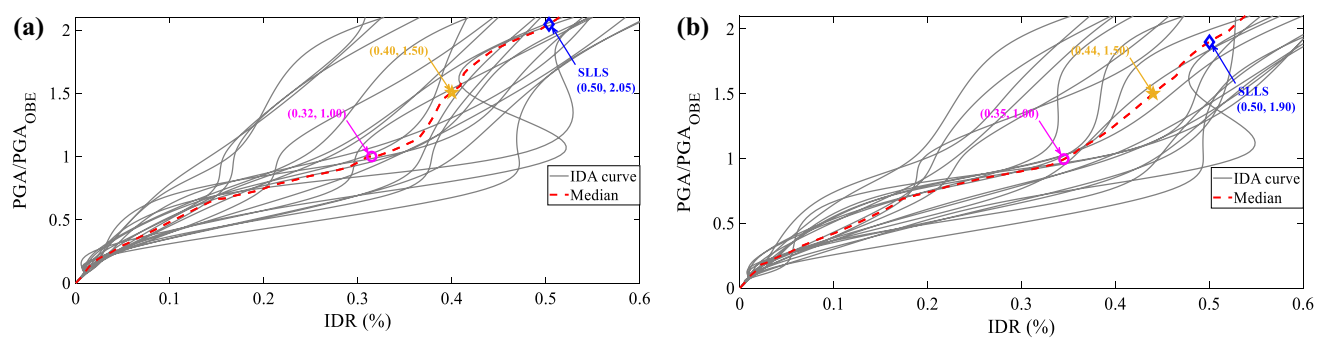

Fig. 11 IDA curves for the normalised seismic intensity as a function of IDR **a** W/O and **b** W/SSI

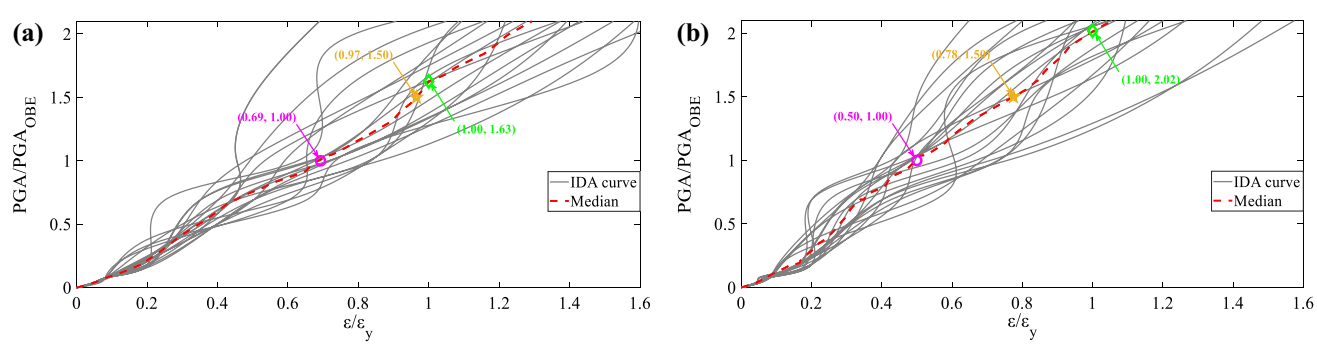

Fig. 12 IDA curves for the normalised seismic intensity as a function of normalised pipe strain **a** W/O and **b** W/SSI

Author's personal copy

Measure (IM). It is a useful tool that can be used to evaluate the seismic vulnerability of new or existing buildings for retrofitting measures and can help engineers to take preemptive actions as well as evaluate the risk and resilience in a quantitative manner. There are several analysis methods for deriving seismic fragility functions for structural systems depending among others on the available number of records, model scale and simplicity of statistical models (Baltzopoulos et al. 2017, Bakalis and Vamvatsikos 2018). In the present study, the Incremental Dynamic Analysis (IDA) (Vamvatsikos and Allin Cornell 2002) was selected in virtue of the relative small model scale, and the ability of the method to account for the record-to-record randomness at various seismic intensities levels, which was necessary due to the mass and strength irregularity as well as dynamic coupling of the system. The IDA was conducted by applying the 20 progressively scaled records starting at $PGA = 0.01$ g with initial step at roughly 0.05 g, whereas the step increased for higher PGA in order to keep the number of scaled records no more than 12. The same stepping algorithm was adopted for the case with SSI. The FFs followed the standard normal cumulative distribution function, which is described by:

$$P\left(EDP > EDP_C | IM = x\right) = \Phi\left(\frac{\ln \frac{x}{IM_{C,50\%}}}{\beta_{tot}}\right) \quad (1)$$

where EDP_C is the upper limit of each damage state, x is the IM that causes exceedance of each limit state, $lnIM_{C,50\,\%}$ is the median μ_{IM} of IMs (or mean of $lnIM$), and β_{IM} is the dispersion of the $lnIM$ that encompasses only the record-to-record variability. Other sources of uncertainty, namely the accuracy in the definition of damage state values and the capacity of the pipe rack (modelling) were not considered because of the deficiency of numerical and experimental data regarding the system under consideration. Assuming the epistemic uncertainty as prescribed by HAZUS (2004) may not be utterly justifiable, since PR–PSs are not common building structures, and thus additional research is needed so as generally acknowledged and valid values to be accounted for the fragility derivation. Apart from the PGA, the fragility was derived for different IMs and these are spectral acceleration and displacement at PR fundamental period (S_{aR}) and pipelines (S_{dP} and S_{dR}), respectively. The highest dispersion due to epistemic uncertainty with respect to pipe rack response was observed for SLS and PGA, and was equal to 0.34, whereas the pertinent value for the pipelines was estimated at 0.52 for SLLS and S_{aR} (Tables 5, 6). The higher dispersion of pipelines in comparison with the PR could be an indication that the selection of period for the spectral acceleration value should be made with due consideration of piping system principal modes and their design should rely on modern methods that could reduce uncertainties. The spectral acceleration was proved a better intensity measure to describe the pipe rack response, since the dispersion $\beta_{d,SaR}$ was considerably lower for all cases (Table 5). In the same vein, the spectral displacement $\beta_{d,SdP}$ estimated at the fundamental period of the pipeline was significantly a better measure for pipelines seismic response than the one at the fundamental period of the pipe rack $\beta_{d,SdR}$, whereas the dispersion was comparable between the LSs with respect to PGA and S_a (Table 6). Due to the lack of literature on the seismic fragility estimation of PRs, it is not feasible to make direct comparisons on the estimated dispersion values, though, they were in good agreement in terms of upper bound with the ones pertaining to common steel frames e.g. see Kazantzi et al. (2014). PS dispersion might be compared with pipelines attached on common or healthcare facilities. The work of Shang et al. (2019) addressed displacement-sensitive pipelines mounted on a base-isolated structure and the dispersion β_d of spectral acceleration at the fundamental period of the structure considering the pipe deformation as EDP was in the 0.45–0.50 interval, which was greater compared to the dispersion that occurred for the examined PS considering spectral measure at the fundamental period of the PS. Strictly speaking, a general conclusion cannot be made given the differences in the seismic response of the healthcare facility and PR.

Table 5 Dispersion β for the pipe rack W/O and W/SSI considering PGA and S_{aR} as IM

Limit state	$\beta_{d,PGA}$	$\beta_{d,SaR}$
SLS		
W/O	0.34	0.21
W/	0.33	0.22
SLLS		
W/O	0.32	0.26
W/	0.31	0.29

Table 6 Dispersion β for the pipelines W/O and W/SSI considering PGA, S_{dR} and S_{dP}

Limit state	$\beta_{d,PGA}$	$\beta_{d,\,SaP}$	$\beta_{d,\,SdR}$	$\beta_{d,SdP}$
SLS				
W/O	0.18	0.30	0.47	0.28
W/	0.36	0.34	0.42	0.38
SLLS				
W/O	0.27	0.36	0.52	0.22
W/	0.40	0.66	0.46	0.32

The FFs for the PR are plotted in Fig. 13 for the SLS and SLLS to keep the seismic intensity up to a practical level. To demonstrate the degree of uncertainty in the fragility estimation, the Standard Error (SE) was plotted for the curves W/O SSI. The error of median capacity was demonstrated

Author's personal copy

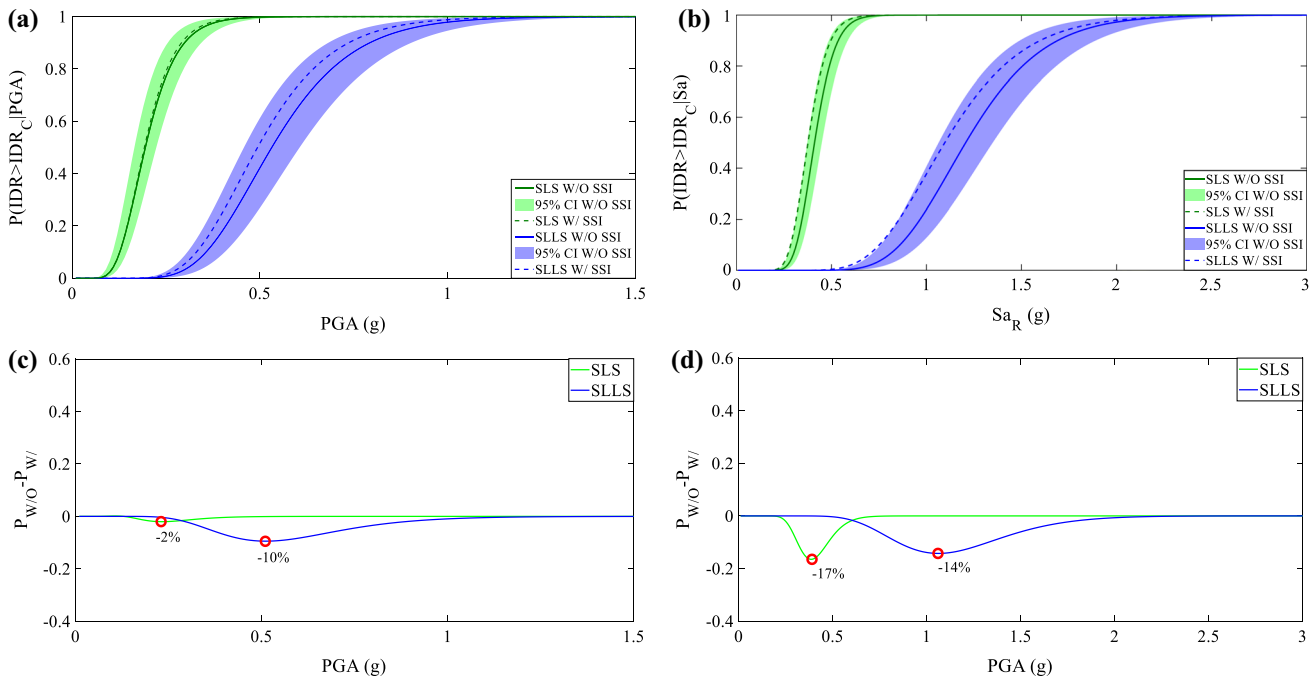

Fig. 13 Fragility analysis of the pipe rack W/O and W/SSI: **a** FFs with IM = *PGA*, **b** FCs with IM = Sa_R as IM, **c**, **d** difference of fragility curves for IM = *PGA* and S_{aR}, respectively

as 95% confidence interval and calculated as a ratio between the sample dispersion over the square root of the sample size (N = 20). The highest SE for the PR and pipes was 8% and 12%, respectively, which means that the median e.g. of *PGA* for the PR and SLLS was within the (0.46 g, 0.61 g) interval with 95% probability. The pertinent interval for the pipes was (0.73 g, 0.82 g). However, it should be kept in mind that the dispersion does not account for aleatory uncertainties that can raise the SE up to 20% when accounting for common dispersion e.g. 0.4 for the accuracy in the definition of LSs and 0.3 for modelling, as proposed in HAZUS (2004). A reliable work that discussed the SE as a function of seismic records number was conducted in Shome and Cornell (1999).

The *PGA* was estimated at 2.05 times greater than the design value, PGA_{OBE}, for the fixed-base case, whereas the deformability of soil was proved detrimental for the PR, reducing the ratio PGA/PGA_{OBE} at 1.90 (Fig. 13a). Concerning the spectral acceleration, the ratio $S_{aR}/S_{aR,d}$ was reduced from 1.84 to 1.67, whilst the reduction for the SLS was obscure (Fig. 13b). It is interesting that the probability of exceedance of SLLS for the PR at PGA_{OBE} was zero for all cases. The difference between the two probabilities is plotted in Fig. 13c and d, where the wider bell curve indicates the higher dispersion observed for the SLLS, and the negative value of difference of two probabilities signifies that the SSI was detrimental. The displacement demand on PR increased particularly at higher seismic intensity, since the period of the system increased by 6% and 14% in the X and Y direction, respectively. The increase of IDR has also been found for other types of steel structures. For instance, Minasidis et al. (2014) observed 15–30% rise on *IDR* due to SSI for a three-storey steel frame of which the increase on the fundamental period was not higher than the one observed for the present PR.

In contrast with the PR, the influence was beneficial for the pipelines (Fig. 14a–c), since the soil acted as a safety pad. In more details, the pipelines yielding was achieved at 0.43 g and 0.53 g (or 1.65 and $2.04 \times PGA_{OBE}$) of *PGA* for the case W/O and W/SSI, respectively, whereas the impact was even greater for the SLLS. Even if the lower confidence bound is considered, the exceedance of the SLS is achieved at 1.5 the PGA_{OBE}, which indicates the system conservativeness. With respect to spectral acceleration, the median value of S_{aP} W/O SSI was 2.64 times greater than the design value, $S_{aR,d}$, and it increased at 4.50 W/SSI. Also, the spectral displacement S_{dP} for the SLLS raised from 0.75 to 1.16 cm and the relevant values were considerably higher in case of S_{dR}. Anew, the difference of probabilities W/O and W/SSI was plotted in Fig. 15a–c and it could easily be noticed that the SLS has a narrow and shorter bell curve, which means that the standard deviation was lower and the effects of SSI were less significant than the SLLS. Among all the cases, the most narrow curve was observed for the S_{dP}, which is another way to confirm the lowest dispersion caused by this IM.

Author's personal copy

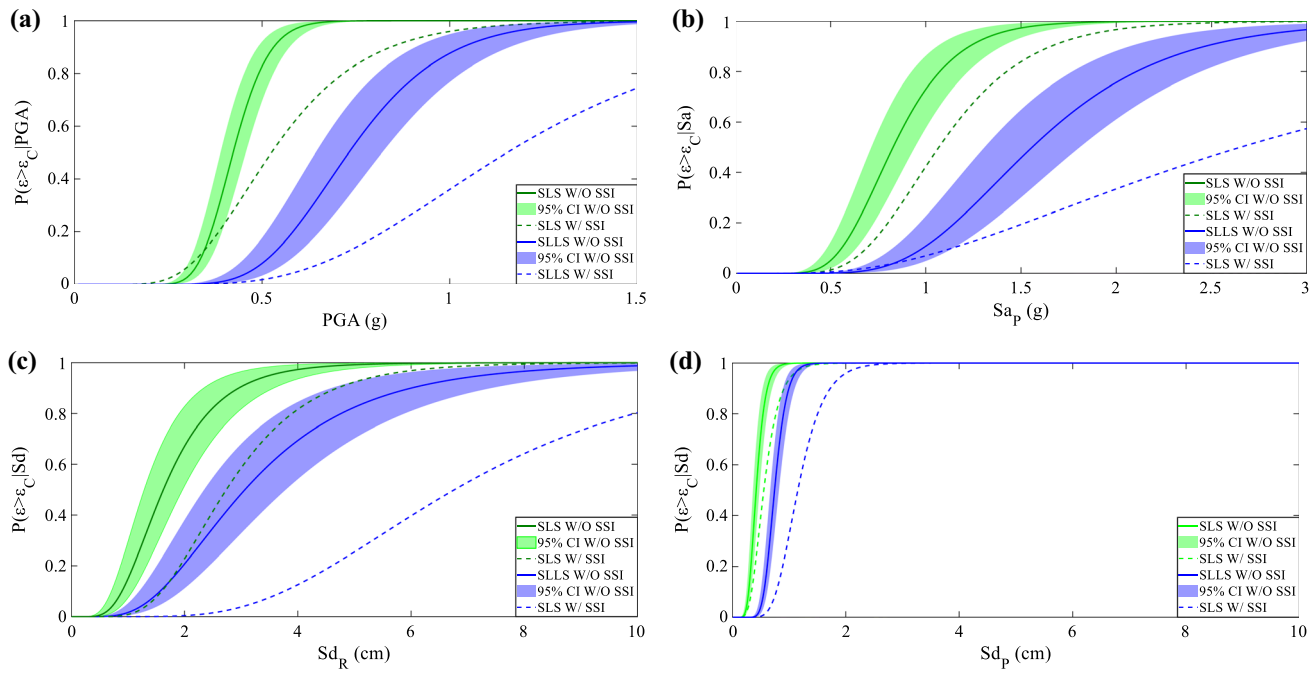

Fig. 14 FFs of pipelines W/O and W/SSI for two LSs considering **a** *PGA*, **b** Sd_R and **c** Sd_P as IM

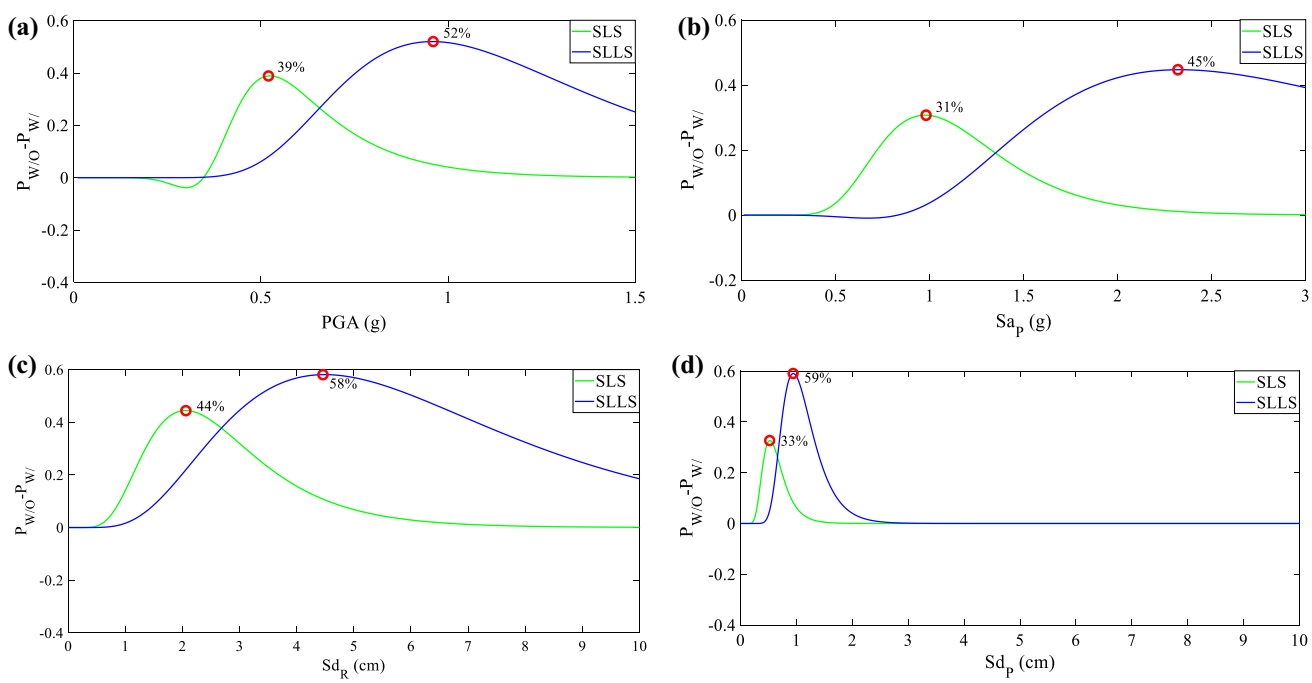

Fig. 15 The difference of FFs of pipelines W/O and W/SSI per each LS considering **a** *PGA* and **b** Sd_R as IM

One might expect that the higher displacements on PR due to SSI could cause higher displacement demand for pipelines as well. Practically, the soil decreased the inertia forces (or acceleration) applied on the PR as an isolation system does, making the flexible components such as pipe and vessels towers to undertake less inertia forces, and thus the PS, which was attached to, was subjected to lower displacements. The influence of soil flexibility on nonstructural components seismic response mounted on a four-storey steel frame was investigated in Raychowdhury

Author's personal copy

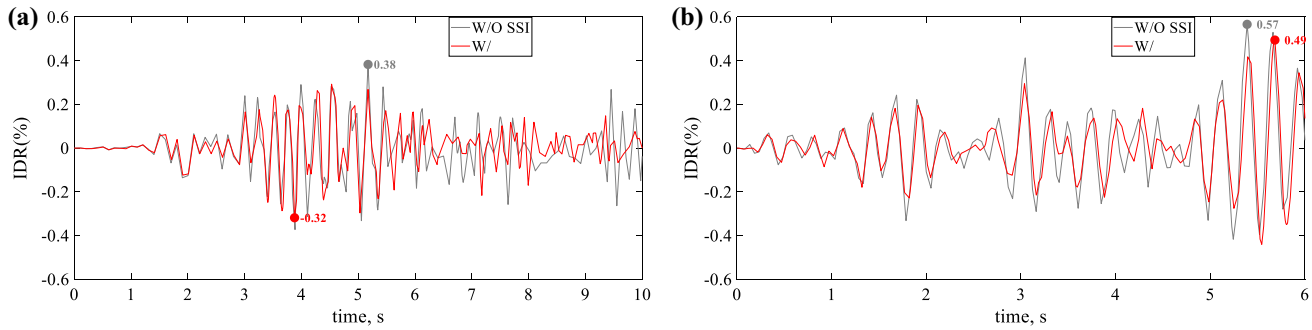

Fig. 16 The IDR time histories of the tower in the Y direction W/O and W/SSI for **a** Rec1 and **b** Rec2 (seismic level nearly 4×SSE)

and Ray-Chaudhuri (2015). Modelling the soil with linear springs was proved to lessen the floor acceleration demand of components close to first fundamental period of the linear fixed-base structure, however, the impact was comparable for components with fundamental periods close to higher modes of vibration of the structure. Also, the higher the seismic intensity of input excitation, the greater the influence of SSI, as it was also demonstrated for the pipelines in the present study.

The IDR time history of the tower that the pipeline is anchored to is presented for the Y direction and two seismic records in Fig. 16, and indeed, the maximum IDR was found lower by 16% and 14%, which could be considerable along with additional decrease of displacement within the PR to reduce the pipeline stresses when incorporating the soil deformability. It should be noted that the Y direction was selected since the pipeline was unrestrained in that direction on the adjacent tower and caused the highest plastic strain on T-joint (see in this respect Fig. 8a and b).

Coming back to the seismic vulnerability of the system, the estimation of mean annual frequency of exceedance of each LS (λ) has been a generally acknowledged estimate within the performance-based design framework. According to Cornell et al. (2002) and Jalayer (2003), λ can be evaluated by integrating the fragility function for each LS with the hazard curve of the site that the structure is located in (Milazzo, northeast part of Sicily, Italy), thus, it holds:

$$\lambda_{LS} = \int_{0}^{+\infty} \frac{dP\left(EDP > EDP_C | IM\right)}{dIM} \cdot H(IM)dIM \tag{2}$$

where H constitutes the function of annual probability of exceedance for a specific IM (hazard function). The integration was conducted for two IMs, namely PGA and S_a, both for PR and pipelines and the results in terms of λ and return period T are quoted in Table 7 and 8. The S_a resulted in smaller λ or greater return period of exceedance of SLS and SLLS with respect to PGA and it seems a more efficient IM in case of PR, given its lower dispersion. In case of pipelines, the two IMs were comparable, and thus further assessment is required accounting for the S_d as well as additional records for higher seismic intensity. The value of λ_{LS} pertains to the observed mean annual frequency of collapse of a LS considering nonlinear response, while typical values of λ postulated in the design codes regard the imposed limit on the hazard. Common values of λ, which are 0.0200, 0.0021 and 0.001 for SLS, SLLS and CLS, respectively, cannot apply, since the PR is part of a critical facility. Considering the pertinent values proposed by NTC (2018) for industrial plants (0.013, 0.0014, 6.8×10^{-4}), all the estimated values of λ_{LS} were smaller; however, the difference was more significant for the S_a and became even greater when pipelines are of concern. Finally, the difference in the return period

Table 7 Mean annual frequency of exceedance (λ_{LS}) and return period of SLS and SLLS for PR considering PGA and Sa_R

λ_{LS}	PGA	T_{PGA}	S_{aR}	T_{SaR}
SLS				
W/O	0.00753	133	0.00155	645
W/	0.00764	131	0.00189	529
SLLS				
W/O	9.8×10^{-4}	1020	1.1×10^{-4}	9091
W/	0.00116	862	1.6×10^{-4}	6667

Table 8 Mean annual frequency of exceedance (λ) and return period of SLS and SLLS for pipelines considering PGA and S_{aP}

λ_{LS}	PGA	T_{PGA}	S_{aP}	T_{SaP}
SLS				
W/O	0.00142	704	3.3×10^{-4}	3030
W/	0.00111	901	1.8×10^{-4}	5556
SLLS				
W/O	4.3×10^{-4}	2326	6×10^{-5}	14286
W/	1.1×10^{-4}	9091	4×10^{-5}	20,000

Author's personal copy

of exceedance, particularly for the SLLS due to SSI, signifies the considerable impact of soil deformability in the vulnerability of the system that should be accounted for in the design phase. The reduction of seismic vulnerability of pipelines due to SSI can be used in the future within the performance-based design context, so that these systems are designed according to modern methods.

5 Conclusions

A performance-based assessment of a steel petrochemical plant pipe rack and piping system was addressed taking the SSI into account and the following deductions are drawn:

- The low values of *IDR* (=0.40% at SSE level) indicated the high stiffness of the pipe rack and the conservativeness of the design according to current code provisions. This outcome was further demonstrated by estimating the mean annual frequency of exceedance of SLLS, which was lower by 92% than the design value considering spectral acceleration, S_{aR}.
- The piping system reserved considerably higher safety than the pipe rack, which reflects the overconservativeness of piping design codes, as it is demonstrated in the current literature. The difference in terms of mean annual frequency of collapse was nearly 96% (anew, the S_{aR} is adopted).
- The soil deformability resulted in adverse effects for the pipe rack and pipelines, and the higher the seismic intensity, the greater the impact for both of them. The ratio $S_{aR}/S_{aR,d}$ that caused exceedance of SLLS reduced from 1.84 to 1.67 for the pipe rack, whilst it increased from 2.64 to 4.50 for the pipelines. Furthermore, the spectral displacement at piping system period, S_{dP}, rose from 0.75 to 1.16 cm.
- The dynamic interaction of the vessels governed the response of the system at high seismic intensity, and this is one reason for the higher seismic vulnerability of the pipe rack compared to the pipes and the greater effect of SSI at higher levels of intensity measure.
- Even though the spectral acceleration S_a yielded lower dispersion compared to *PGA* for the pipe rack, the selection of appropriate measure for the pipelines seems more challenging. To this effect, spectral acceleration and displacement were both considered, and indeed, the latter measure caused lower dispersion of response parameter when it was evaluated at piping system fundamental period.
- Finally, the high dispersion for the SLLS may also be derived by the modest amount of records that raised the standard error of estimation of sample median at 12% for the pipes .

The present study intended to shed some light on pipe rack—piping systems seismic response towards designing them according to modern methods. Idiosyncrasies of the system concerning the adverse effects of soil and degree of conservativeness of design codes on structural and non-structural members were illustrated. In virtue of the assumptions made e.g. linear soil modelling, boundary conditions or number of records, the results cannot be generalised and thus further numerical and experimental research is required.

Acknowledgements The work presented herein has received funding from the European Union's Horizon 2020 research and innovation programme under the Marie Sklodowska-Curie Grant Agreement No 721816. This support is gratefully acknowledged.

References

ABAQUS. (2017). ABAQUS/Standard Version 6.17, Documentation, Dassault Systèmes, Providence, RI, USA.

Azizpour, O., & Hosseini, M. (2009). A verification study of ASCE recommended guidelines for seismic evaluation and design of combination structures in petrochemical facilities. *Journal of Applied Sciences, 9*(20), 3609–3628. https://doi.org/10.3923/jas.2009.3609.3628.

Bakalis, K., & Vamvatsikos, D. (2018). Seismic Fragility Functions via Nonlinear Response History Analysis. *Journal of Structural Engineering (United States)*. https://doi.org/10.1061/(ASCE)ST.1943-541X.0002141.

Baltzopoulos, G., et al. (2017). SPO2FRAG: Software for seismic fragility assessment based on static pushover. *Bulletin of Earthquake Engineering*. https://doi.org/10.1007/s10518-017-0145-3.

Bhattacharya, K., Dutta, S. C., & Dasgupta, S. (2004). Effect of soil-flexibility on dynamic behaviour of building frames on raft foundation. *Journal of Sound and Vibration*. https://doi.org/10.1016/S0022-460X(03)00652-7.

Bursi, O. S., et al. (2015). Performance-based earthquake evaluation of a full-scale petrochemical piping system. *Journal of Loss Prevention in the Process Industries, 33,* 10–22. https://doi.org/10.1016/j.jlp.2014.11.004.

Bursi, O. S., et al. (2016). Seismic assessment of petrochemical piping systems using a performance-based approach. *Journal of Pressure Vessel Technology, Transactions of the ASME*. https://doi.org/10.1115/1.4032111.

Cornell, C. A., et al. (2002). Probabilistic basis for 2000 SAC federal emergency management agency steel moment frame guidelines. *Journal of Structural Engineering, 128*(4), 526–533. https://doi.org/10.1061/(ASCE)0733-9445(2002)128:4(526).

DeGrassi, G., Nie, J., & Hofmayer, C. (2008) *Seismic analysis of large-scale piping systems for the JNES-NUPEC ultimate strength piping test program*. Retrieved from https://scholar.google.com/scholar?hl=en&btnG=Search&q=intitle:Seismic+Analysis+of+Large-Scale+Piping+Systems+for+the+Ultimate+Strength+Piping+Test+Program#1. Accessed 5 Dec 2018.

Di Roseto, A. D. L., Palmeri, A., & Gibb, A. G. (2017). Performance-based seismic design of a modular pipe-rack. *Procedia Engineering*. https://doi.org/10.1016/j.proeng.2017.09.519.

Di Sarno, L., & Karagiannakis, G. (2019). Petrochemical steel pipe rack: Critical assessment of existing design code provisions and a case study. *International Journal of Steel Structures*. https://doi.org/10.1007/s13296-019-00280-w.

Author's personal copy

Dutta, S. C., Bhattacharya, K., & Roy, R. (2009). Effect of flexibility of foundations on its seismic stress distribution. *Journal of Earthquake Engineering*. https://doi.org/10.1080/13632460802211974.

Elnashai, A. S., & Di Sarno, L. (2015). *Fundamentals of earthquake engineering: From source to fragility*. Second: Wiley. https://doi.org/10.1002/9780470024867.fmatter/pdf.

EN13480-3. (2012). EN 13480-3, 2002, Metallic Industrial Piping–Part 3: Design and Calculation, CEN, Brussels.

EN1998-1. (2004). Eurocode 8: Design of structures for earthquake resistance—Part 1 : General rules, seismic actions and rules for buildings, European Committee for Standardization. doi: [Authority: The European Union per Regulation 305/2011, Directive 98/34/EC, Directive 2004/18/EC].

FEMA 356. (2000). Prestandard and Commentary for the Seismic Rehabilitation of Building, Federal Emergency Management Agency.

Gazetas G. (1991). Foundation vibrations. In H. Y. Fang (Ed.), *Foundation engineering handbook*. Boston, MA: Springer. https://doi.org/10.1007/978-1-4615-3928-5_15.

HAZUS. (2004). National Institute of Building Sciences. Direct physical damage—general building stock, HAZUS-MH Technical manual, chapter 5. Federal Emergency Management Agency, Washington, D.C.

Jalayer, F. (2003). Direct probabilistic seismic analysis: implementing non-linear dynamic assessments. Department of Civil and Environmental Engineering, Ph.D.

Kazantzi, A. K., Vamvatsikos, D., & Lignos, D. G. (2014). Seismic performance of a steel moment-resisting frame subject to strength and ductility uncertainty. *Engineering Structures*. https://doi.org/10.1016/j.engstruct.2014.06.044.

Minasidis, G., Hatzigeorgiou, G. D., & Beskos, D. E. (2014). SSI in steel frames subjected to near-fault earthquakes. *Soil Dynamics and Earthquake Engineering*. https://doi.org/10.1016/j.soildyn.2014.06.030.

Mylonakis, G., & Gazetas, G. (2000). Seismic soil-structure interaction: Beneficial or detrimental? *Journal of Earthquake Engineering, 4*3, 277–301. https://doi.org/10.1080/13632460009350372.

NTC. (2018). Norme Tecniche per le costruzioni. DM Infrastructure, 14 January. (**in Italian**).

Raychowdhury, P., & Ray-Chaudhuri, S. (2015). Seismic response of nonstructural components supported by a 4-story SMRF: Effect of nonlinear soil-structure interaction. *Structures*. https://doi.org/10.1016/j.istruc.2015.04.006.

Shang, Q., Wang, T., & Li, J. (2019). Seismic fragility of flexible pipeline connections in a base isolated medical building. *Earthquake Engineering and Engineering Vibration*. https://doi.org/10.1007/s11803-019-0542-5.

Shome, N. & Cornell, C. A. (1999). Probabilistic Seismic Demand Analysis of Nonlinear Structures. Report No. RMS-35. Reliability of Marine Structures Program, Department of Civil and Environmental Engineering, Stanford University.

Vamvatsikos, D., & Allin Cornell, C. (2002). Incremental dynamic analysis. *Earthquake Engineering and Structural Dynamics, 31*(3), 491–514. https://doi.org/10.1002/eqe.141.

Vathi, M., et al. (2017). Performance criteria for liquid storage tanks and piping systems subjected to seismic loading. *Journal of Pressure Vessel Technology. doi, 10*(1115/1), 4036916.

Wang, X., et al. (2017). Analysis of seismic soil-structure interaction for a nuclear power plant (HTR-10). *Science and Technology of Nuclear Installations*. https://doi.org/10.1155/2017/2358403.

Zhang, C., & Jiang, N. (2017). Effects of equipment-structure-soil interaction on seismic response of equipment and structure via real-time dynamic substructuring shaking table testing. *Shock and Vibration*. https://doi.org/10.1155/2017/1291265.

Publisher's Note Springer Nature remains neutral with regard to jurisdictional claims in published maps and institutional affiliations.